Available online at www.sciencedirect.com

ScienceDirect

Journal of Natural Gas Geoscience 3 (2018) 157−169

http://www.keaipublishing.com/jnggs

Original research paper

Study on the influence of elastic modulus heterogeneity on in-situ stress and its damage to gas shale reservoirs☆

Daobing Wang [a,b], Hongkui Ge [c,*], Bo Yu [a], Dongsheng Wen [b], Jun Zhou [d], Dongxu Han [a], Lu Liu [e]

[a] School of Mechanical Engineering, Beijing Key Laboratory of Pipeline Critical Technology and Equipment for Deepwater Oil & Gas Development, Beijing Institute of Petrochemical Technology, Beijing 102617, China

[b] School of Aeronautic Science and Engineering, Beihang University, Beijing 100083, China

[c] The Unconventional Natural Gas Institute, China University of Petroleum, Beijing 102249, China

[d] Sinopec Research Institute of Petroleum Engineering, Beijing 100101, China

[e] Chongqing Gas Mine of Southwest Oil and Gas Field Branch, CNPC, Chongqing 400021, China

Received 23 March 2018; revised 8 June 2018

Available online 31 August 2018

Abstract

Shale heterogeneity has a significant effect on drilling and completions, hydraulic fracturing, as well as hydrocarbon development performance. However, it lacks representation of rock damage/failure caused by the mechanical heterogeneity and “stress shadow” effect during the hydraulic fracturing process. In this paper, the Galerkin finite element method was adopted to numerically simulate the hydro-mechanical coupled interaction based on the solver in the COMSOL Multiphysics software and Matlab scripting development. The Weibull probability density function was used to represent the mechanical heterogeneity of gas shale. Under the condition of fully fluid-solid coupling during the fracking process, the effect of mechanical heterogeneity on von − Mises stress, strain energy density, damage factor, and fluid pressure was numerically simulated in the gas shale wells. The curves of von − Mises stress, strain energy density, and damage factor along a certain straight line showed the obvious decreasing distribution in a completely homogeneous formation. As the strata are heterogeneously enhanced, their distribution curves showed fluctuations. Moreover, von − Mises stress and strain energy density had a good relationship with damage factors. Accordingly, the method of rock damage/fracture and "stress shadow" effect caused by mechanic heterogeneity was put forward under the circumstance of two−dimensional plane strain. That was to use, the von − Mises stress or strain energy density at the single point or line to characterize the degree of local rupture or the shadow effect of stress, and the average strain energy density per unit area to characterize the degree of rupture of the rock or the intensity of the shadow effect. The study is of great significance to further improve the SRV(Stimulated Reservoir Volume) fracturing design and the productivity of gas shale wells.

1. Introduction

Rock heterogeneity is a property that reservoir property varies in regards to its spatial location. The value of the damage variable is closely related to the heterogeneous parameter when rock failure occurs. Meanwhile, the agglomeration and release of elastic energy during the failure process are closely related to heterogeneity. The shale itself is also a source rock, and the solid organic matter still exists in the rock after generating gas. The shale has strong heterogeneity since the organic matter is oil-wet and unevenly distributed in the formation. The heterogeneity of shale has a significant impact on these processes: drilling and completion, hydraulic fracturing, and gas reservoir development.

☆ This is English translational work of an article originally published in *Natural Gas Geoscience* (in Chinese). The original article can be found at:10.11764/j.issn.1672-1926.2018.04.001.

* Corresponding author.

E-mail address: gehongkui@163.com (H. Ge).

Peer review under responsibility of Editorial office of *Journal of Natural Gas Geoscience*.

https://doi.org/10.1016/j.jnggs.2018.08.002

Zhu et al. [1] established a rock-isotropic THM(Thermo-Hydro-Mechanical) damage coupling model that considers the effects of rock damage on temperature, seepage, and stress field distribution. Wei [2] considered the influence of coal desorption deformation and temperature change on methane content. The said researcher also studied the damage model of coal rock under the condition of thermo-hydro-mechanical (THM) coupling and simulated the evolution law of the coal rock damage zone. Lu et al. [3] wrote the program of rock damage and seepage process under fluid-solid coupling. They numerically simulated the damage evolution law of coal floor cracks on the top of water-pressured in coal mining process. According to the transversely isotropic constitutive equation, Wang et al. [4] established a damage model with consideration of the seepage-stress-chemical coupling and analyzed the hydration characteristics of the layered rock. Mi [5] considered the concrete mesostructure model and developed a plastic model program for the damage evolution of concrete components. Zhu et al. [6] considered the mesoscopic heterogeneity of rock, proposed a micromechanical model of rock deformation and failure, and developed the famous RFPA program. The simulation results present that the homogenization parameter is the most crucial factor that affects rock failure. Wang et al. [7] simulated the damage evolution law of shale gas wells during gas fracturing. The crack initiation pressure, fracturing pressure, and fracture complexity decrease with increasing interface tension and dynamic viscosity. Based on the fluid-solid coupling modeling method in continuum mechanics, Lu et al. [8] proposed a two-scale conceptual model to represent real rock materials with micro-cracks. Combined with the Biot pore-elastic theory, the continuous damage evolution process of micro-cracks was numerically simulated. The crack initiation pressure and the fracturing pressure decrease with increasing permeability. Nonetheless, the aforementioned increases with the increasing wellbore pressurization rate. Pogacnik et al. [9] introduced the micro-mixing rupture criterion based on the energy release rate into the hydraulic fracturing damage mechanics model of the enhanced geothermal system. The results show that the failure mode near the wellbore zone transits from shear failure to tensile failure mode with increasing flow pressure. It is also worth noting that the said occasion, the rock damage increased rapidly.

Although the former [1−6] used the Weibull random function to represent the heterogeneity of the rock and used the damage mechanics method to simulate the rock rupture and seepage process, there is no effective characterization method to describe the heterogeneity. The rock damage/fracture, "stress shadow" effect, as well as the influence law of various factors (i.e., the degree of heterogeneity and the variable energy density) are not analyzed in detail. Through the COMSOL Multiphysics solver, the authors used the Matlab high-level language to carry out secondary development. The Galerkin finite element method was used to simulate the influence of heterogeneity on rock stress distribution, strain energy density, flow pressure, and damage factor under fluid-solid coupling conditions. The characterization method of rock damage/rupture and "stress shadow" effect caused by heterogeneity is given. This study has an essential guiding significance that can aid the further improvement of shale volume fracturing design and gas well productivity.

2. The physical model

There is a vertical well in the formation, and the physical model of the wellbore hydraulic fracturing is shown in Fig. 1. The assumptions are as follows:

(1) The formation permeability is isotropic. That is, the permeability values in the horizontal direction and the vertical direction are the same.
(2) Due to the great thickness of the reservoir, the three-dimensional complication can be simplified into a two-dimensional plane strain problem.
(3) The maximum and minimum horizontal principal stresses in the far field are respectively denoted as σ_1 and σ_3.
(4) The flow pressure acting on the well wall is denoted as p_w.
(5) It is assumed that the geostress equilibrium is carried out under the conditions of formation temperature; the process of rock deformation is an isothermal process.
(6) The original pore pressure in the formation is denoted as p_p. The formation fluid is slightly compressible, and the influence of fluid-solid coupling effect on the distribution of in-situ stress and pore pressure is considered.
(7) The rock pressure damage caused by the changes in flow pressure and rock deformation is considered.

3. The mathematical model

3.1. Governing equations

Assuming that the problem satisfies the two-dimensional plane strain condition, the stress tensor and the strain tensor are expressed in vector form as follows [10−13]:

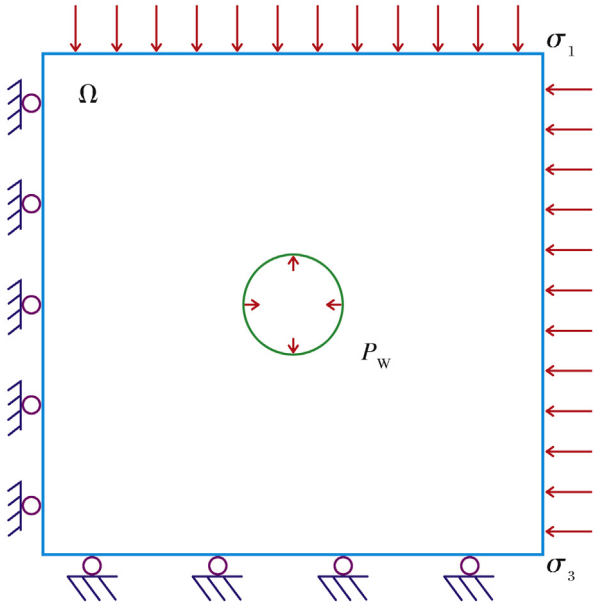

Fig. 1. The physical model of hydraulic fracturing for vertical wells.

$$\boldsymbol{\sigma} = \left\{\sigma_x, \sigma_y, \tau_{xy}\right\}^T \tag{1}$$

$$\boldsymbol{\varepsilon} = \left\{\varepsilon_x, \varepsilon_y, \gamma_{xy}\right\}^T \tag{2}$$

Considering the isothermal equilibrium and ignoring the volume force under the assumption of the small rock deformation theory, the rock stress equilibrium equation is as follows:

$$\mathbf{L}^T\boldsymbol{\sigma} + \rho\mathbf{g} = \mathbf{0} \tag{3}$$

where differential operator $\mathbf{L} = \begin{bmatrix} \frac{\partial}{\partial x} & 0 & 0 \\ 0 & \frac{\partial}{\partial y} & 0 \\ \frac{\partial}{\partial y} & \frac{\partial}{\partial x} & 0 \end{bmatrix}$; $\rho = (1-\varphi)\rho_s + \varphi\rho_w$; φ denotes rock porosity. Meanwhile, ρ_s and ρ_w respectively denote the density of rocks and fluids, and $\boldsymbol{g}$ denotes the acceleration of gravity.

According to Darcy's law, the single-phase fluid pressure equation in rock is as follows

$$\left(\frac{\alpha-\varphi}{K_s} + \frac{\varphi}{K_w}\right)\frac{\partial p_w}{\partial t} + \alpha\mathbf{m}_v^T\frac{\partial\boldsymbol{\varepsilon}}{\partial t} + div\left[\frac{\mathbf{k}}{\mu_w}(-gradp_w + \rho\mathbf{g})\right] = 0 \tag{4}$$

where K_s and K_w denote the bulk moduli of rock skeleton and liquid respectively. The μ_w denotes the fluid viscosity, $\boldsymbol{k}$ denotes the formation permeability tensor, p_w denotes the fluid pressure, and α denotes the Biot elastic coefficient, $\alpha \in [0,1]$; $\mathbf{m}_v^T = [1,1,1,0,0,0]^T$.

According to the relationship between the strain tensor and displacement vector, the following can be achieved:

$$d\boldsymbol{\varepsilon} = \mathbf{L}d\mathbf{u} \tag{5}$$

According to the definition of effective stress, the relationship between effective stress $\boldsymbol{\sigma}''$ and total stress $\boldsymbol{\sigma}$ is as follows:

$$\boldsymbol{\sigma} = \boldsymbol{\sigma}'' - \alpha\mathbf{m}_v p_w \tag{6}$$

According to the linear elastic assumption, the effective stress–strain constitutive relation is as follows:

$$d\boldsymbol{\sigma}'' = \mathbf{D}_T d\boldsymbol{\varepsilon} \tag{7}$$

where $\mathbf{D}_T$ denotes the tangential constitutive tensor.

3.2. Initial and boundary conditions

In the conditions, Ω serves as the domain, the boundary is denoted by Γ, $\boldsymbol{n}_v$ is the normal boundary vector, the displacement and traction acting on the boundary are respectively $\widehat{\mathbf{u}}$ and $\bar{\mathbf{t}}$, and the pressure and flow rate acting on the boundary are respectively $\widehat{p}_w$ and q_w. The initial conditions and boundary conditions are defined respectively:

3.2.1. Initial conditions

$$\mathbf{u} = \mathbf{u}_0,\ p_w = p_{0w} \tag{8}$$

3.2.2. Boundary conditions

The first type of boundary conditions (i.e., the displacement and pressure boundary conditions) is defined as follows:

$$\mathbf{u} = \widehat{\mathbf{u}},\ p_w = \widehat{p}_w \tag{9}$$

The second type of boundary conditions, namely the traction and flow rate boundary conditions, are defined as follows:

$$\mathbf{I}^T\boldsymbol{\sigma} = \bar{\mathbf{t}} \tag{10}$$

$$\rho_w\frac{\mathbf{k}}{\mu_w}(-gradp_w + \rho_w\mathbf{g})^T\cdot\mathbf{n}_v = q_w \tag{11}$$

where $\mathbf{I} = \begin{bmatrix} n_x & 0 \\ 0 & n_y \\ n_y & n_x \end{bmatrix}$.

3.3. Finite element discretization method

3.3.1. Variational form

According to the finite element variational theory where Ω is the region in Fig. 1, and for any test function $\boldsymbol{w}$ and $\boldsymbol{w}^*$, the variational form of the stress equilibrium equation and the fluid pressure equation is as follows [10–13]:

$$\int_\Omega (\mathbf{L}\mathbf{w})^T\boldsymbol{\sigma}d\Omega = \int_\Omega \mathbf{w}^T\rho\mathbf{g}d\Omega + \int_{\Gamma_u^q}\mathbf{w}^T\bar{\mathbf{t}}d\Gamma \tag{12}$$

$$\int_\Omega\left[-\left(\nabla\mathbf{w}^*\right)^T\left(-\frac{\mathbf{k}}{\mu_w}\nabla p_w + \frac{\mathbf{k}}{\mu_w}\rho_w\mathbf{g}\right) + \mathbf{w}^{*T}\alpha\mathbf{m}_v^T L\frac{\partial\mathbf{u}}{\partial t} + \mathbf{w}^{*T}\left(\frac{\alpha-\varphi}{K_s} + \frac{\alpha-\varphi}{K_w}\right)\frac{\partial p_w}{\partial t}\right]d\Omega + \int_{\Gamma_w^q}\mathbf{w}^{*T}\frac{q_w}{\rho_w}d\Gamma = 0 \tag{13}$$

where Γ_u^q and Γ_w^q respectively correspond to the traction boundary conditions and the flow rate boundary conditions in the boundary Γ.

3.3.2. Galerkin space discretization of governing equations

For this junction, $\mathbf{N}_u$ and $\mathbf{N}_p$ are the displacement shape function and the pressure shape function, respectively. The displacement vector and pressure can be expressed as:

$$\mathbf{u} = \mathbf{N}_u\bar{\mathbf{u}},\ p_w = \mathbf{N}_p\bar{\mathbf{p}}_w \tag{14}$$

where $\bar{\mathbf{u}}$ and $\bar{\mathbf{p}}_w$ are the vectors of the node values of the displacement and pressure on the element. Substituting equation (14) into equations (12) and (13), and taking $\mathbf{w} = \mathbf{N}_u$, $\mathbf{w}^* = \mathbf{N}_p$, so as to obtain:

$$\begin{bmatrix} \mathbf{0} & \mathbf{0} \\ \mathbf{Q}^{\mathbf{T}} & \mathbf{S} \end{bmatrix} \frac{d}{dt}\begin{Bmatrix} \bar{\mathbf{u}} \\ \bar{\mathbf{p}}_w \end{Bmatrix} + \begin{bmatrix} \mathbf{K} & -\mathbf{Q} \\ \mathbf{0} & \mathbf{H} \end{bmatrix}\begin{Bmatrix} \bar{\mathbf{u}} \\ \bar{\mathbf{p}}_w \end{Bmatrix} = \begin{Bmatrix} \mathbf{f}^u \\ \mathbf{f}^p \end{Bmatrix} \tag{15}$$

where the left-hand side matrix:

$$\mathbf{B} = \mathbf{L}\mathbf{N}_u,\quad \mathbf{K} = \int_\Omega \mathbf{B}^T\mathbf{D}\mathbf{B}d\Omega,\quad \mathbf{Q} = \int_\Omega \mathbf{B}^T\alpha\mathbf{m}_v\mathbf{N}_p d\Omega,$$

$$\mathbf{H} = \int_\Omega (\nabla\mathbf{N}_p)^T\frac{\mathbf{k}}{\mu_w}\nabla\mathbf{N}_p d\Omega\,,$$

$$\mathbf{S} = \int_\Omega \mathbf{N}_p^T\left(\frac{\alpha-\varphi}{\mathbf{K}_s} + \frac{\varphi}{\mathbf{K}_w}\right)\mathbf{N}_p d\Omega$$

moreover, the right-hand side matrix:

$$\mathbf{f}^u = \int_\Omega \mathbf{N}_u^T[\rho_s(n-1) + \rho_w n]\mathbf{g}d\Omega + \int_{\Gamma_u^q}\mathbf{N}_u^T\bar{\mathbf{t}}d\Gamma\,,$$

$$\mathbf{f}^p = \int_\Omega (\nabla\mathbf{N}_p)^T\frac{\mathbf{k}}{\mu_w}\rho_w\mathbf{g}d\Omega - \int_{\Gamma_w^q}\mathbf{N}_p^T\frac{q_w}{\rho_w}d\Gamma$$

3.3.3. Time discretization of governing equations

For this part, $\mathbf{X} = \{\bar{\mathbf{u}}, \bar{\mathbf{p}}_w\}^T$, then equation (15) can be expressed as:

$$\mathbf{B}\frac{d\mathbf{X}}{dt} + \mathbf{C}\mathbf{X} = \mathbf{F} \tag{16}$$

According to the finite difference discrete format, the first derivative of time in equation (16) can be approximated as:

$$\left(\frac{d\mathbf{X}}{dt}\right)_{n+\theta} = (\mathbf{X}_{n+1} - \mathbf{X}_n)/\Delta t, \mathbf{X}_{n+\theta} = (1-\theta)\mathbf{X}_n + \theta\mathbf{X}_{n+1} \tag{17}$$

where $0 \le \theta \le 1$, and Δt denotes a time step. Additionally, $\mathbf{X}_n$ and $\mathbf{X}_{n+1}$ represents a vector value at the time t_n and time t_{n+1}, respectively.

Substituting equation (17) into equation (16), the following can be achieved:

$$[\mathbf{B} + \theta\Delta t\mathbf{C}]\mathbf{X}_{n+\theta} = [\mathbf{B} - (1-\theta)\Delta t C]\mathbf{X}_n + \Delta t\mathbf{F}_{n+\theta} \tag{18}$$

Therefore, the time discretization of equation (15) is as follows [10–13]:

$$\begin{bmatrix} \theta\mathbf{K} & -\theta\mathbf{Q} \\ \mathbf{Q}^T & \mathbf{S} + \Delta t\theta\mathbf{H} \end{bmatrix}_{n+\theta}\begin{Bmatrix} \bar{\mathbf{u}} \\ \bar{\mathbf{p}}_w \end{Bmatrix}_{n+1} = \begin{bmatrix} (\theta-1)\mathbf{K} & (1-\theta)\mathbf{Q} \\ \mathbf{Q}^{\mathbf{T}} & \mathbf{S} - \Delta t(1-\theta)\mathbf{H} \end{bmatrix}_{n+\theta}\begin{Bmatrix} \bar{\mathbf{u}} \\ \bar{\mathbf{p}}_w \end{Bmatrix}_n + \begin{Bmatrix} \mathbf{f}^u \\ \Delta t\mathbf{f}^p \end{Bmatrix}_{n+\theta} \tag{19}$$

3.4. The definition of rock damage factor D

The definition of rock damage factor as proposed by Zhu et al. is as follows [1,6]:

$$\mathrm{D} = \begin{cases} 0 & ,\ F_1 < 0, F_2 < 0 \\ 1 - \left|\dfrac{\varepsilon_{t0}}{\varepsilon_3}\right|^2 & ,\ F_1 = 0, dF_1 > 0 \\ 1 - \left|\dfrac{\varepsilon_{c0}}{\varepsilon_1}\right|^2 & ,\ F_2 = 0, dF_2 > 0 \end{cases} \tag{20}$$

where $F_1 = -\sigma_3 - f_{t0}, F_2 = \sigma_1 - \sigma_3\frac{1+\sin\phi}{1-\sin\phi} - f_{c0}$; ϕ denotes the internal friction angle of the rock; f_{t0} and f_{c0} denote the tensile strength and uniaxial compressive strength of the rock, respectively; σ_1 and σ_3 respectively denote the maximum and minimum principal stresses; ε_1 and ε_3 denote the maximum and minimum principal strain, respectively; ε_{t0} and ε_{c0} respectively denote the maximum tensile principle strain and maximum compressive principle strain when the tensile damage and shear damage occurs inside the rock.

According to the theory of damage mechanics, the elastic modulus of an element is defined as follows [1,6]:

$$E = (1-D)E_0 \tag{21}$$

where E and E_0 represent the corresponding elastic modulus values before and after the rock damage, respectively.

3.5. The definition of rock heterogeneity

The initial elastic modulus of the rock serves as a random variable that obeys the Weibull distribution, and the shape parameter m denotes its homogeneity. The Weibull distribution probability density function is defined as follows [1,6]:

$$f(x,m,n) = \begin{cases} \dfrac{m}{n}\left(\dfrac{x}{n}\right)^{m-1} e^{-\left(\frac{x}{n}\right)^m} & ,\ x \ge 0 \\ 0 & ,\ x < 0 \end{cases} \tag{22}$$

where x denotes a random variable, and the parameter represents the elastic modulus that satisfies the distribution in the equation above. The m is the shape parameter, and n is the parameter average. The shape parameter m represents the degree of homogeneity of the random variable x. The smaller

the m value, the weaker the homogeneity. Oppositely, the higher the m value, the stronger the homogeneity. The parameter n represents the average value of the random variable x, and the larger the n value, the larger the average value of x is. As shown in Fig. 2, it is the corresponding rock elastic modulus plane distribution for when the shape parameter is $m = 5$ and the elastic modulus average value is $n = 34.5$ GPa.

3.6. Model verification

According to the theory of rock mechanics, when the reservoir is homogeneous, there is an analytical solution for the stress field around the wellbore [2]. In reference to the necessary parameters in Table 1, the analytical solution of the S_{xx} stress field component and the finite element numerical solution in section 3.3 are calculated when the bottom hole pressure is 30, 40, and 50 MPa, respectively [12–19] (Fig. 3). As shown in Fig. 3, it is found that the two solutions have a good agreement, which verifies the reliability of the finite element numerical solution under the fluid-solid coupling condition.

4. Simulation results

The basic input parameters of the numerical simulation are shown in Table 1. In order to analyze the effects of shale mechanical heterogeneity on geo-stress distribution and rock damage, the parameters of shape parameters m to geo-stress, strain energy density, fluid pressure, and rock damage factor are simulated. The corresponding influence law was analyzed. The details are as follow:

4.1. The influence of heterogeneity on the distribution of geo-stress

The equivalent stress (von − Mises stress) is a yield criterion, and the value of the yield criterion is usually called the equivalent stress. The von − Mises criterion is a comprehensive concept that considers the first, second, and third principal stresses. The above can be used to evaluate fatigue, damage, etc., and is a mechanical concept in elasto-plastic mechanics. It follows the fourth strength theory of material mechanics (shape change specific energy theory). Therefore, the distribution of the von − Mises stress at different levels of degrees of heterogeneity with homogeneity, and different shape parameters $m = 1$, 3 and 5, is simulated as shown in Fig. 4 accordingly. The geo-stress is mainly concentrated near the wellbore if the formation is homogeneous under the action of flow pressure on the wellbore. When the shape parameter m changes from one to five, the formation heterogeneity gradually decreases. The formation heterogeneity in Fig. 4b and c is stronger than others. Moreover, the higher geo-stress occurs near the wellbore. In Fig. 4c, the heterogeneity is relatively weak, and the ground stress is mainly concentrated near the wellbore, which is similar to Fig. 4a. If the shale mechanical heterogeneity is strong, there

Table 1
Basic input parameters.

Parameters	Value
Porosity/dimensionless	0.05
Poisson's ratio/dimensionless	0.25
Young's modulus/GPa	34.5
Rock density/(kg/m^3)	2500
Rock permeability/mD	0.001
Tensile strength/MPa	6.04
Uniaxial compressive strength/MPa	100
Internal friction angle of rock/°	33.7
Damage evolution coefficient/dimensionless	2
Fluid density/(kg/m^3)	1020
Fluid compressibility/(1/Pa)	2×10^{-10}
Fluid viscosity/(mPa·s)	1.8
Initial formation pressure/MPa	28
Maximum horizontal stress in the far field/MPa	40
Minimum horizontal stress in the far field/MPa	30
Hole radius/m	0.1
Injection time/s	60

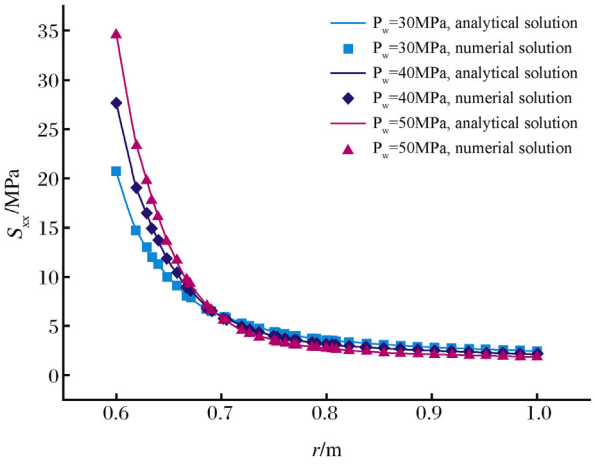

Fig. 3. The comparison of numerical and analytical solutions of S_{xx} stress component.

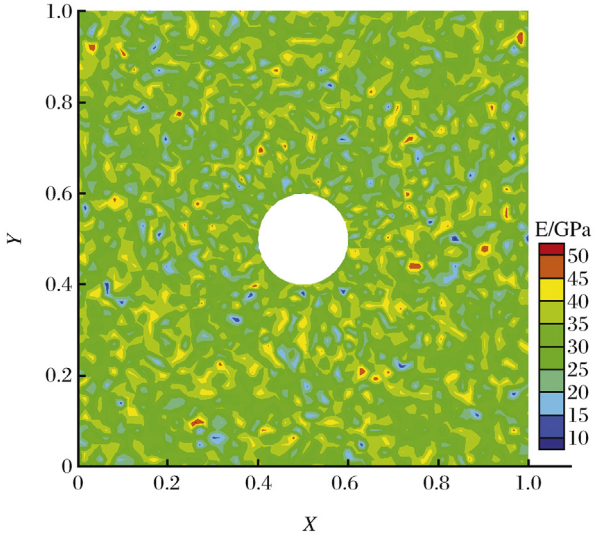

Fig. 2. The 2D distribution of elastic modulus.

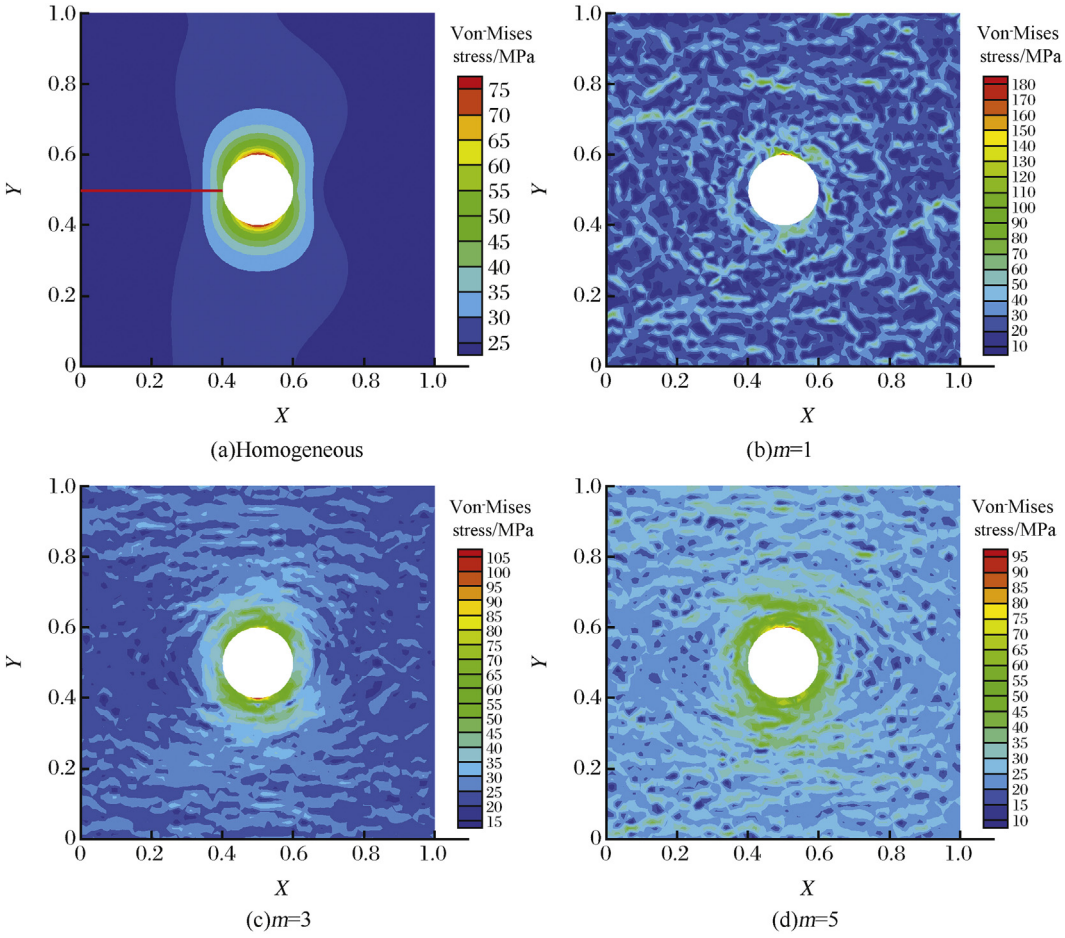

Fig. 4. The 2D distribution figure of von − Mises stress at different levels of shape parameters *m*.

is a high-stress area away from the wellbore, and the probability of rock damage or failure will increase.

According to the results of Fig. 4, the geo-stress distribution maps at different levels of shape parameters *m* are plotted (Fig. 5) along the *x*-axis' forward direction as shown by the red line path in Fig. 4a. When $m = 1$, the formation heterogeneity is strong, the geo-stress fluctuates and is distributed along the path from the borehole wall to the right boundary. With the increase of the value of *m*, the formation heterogeneity is weakened. Furthermore, the geo stress gradually decreases. It indicates that when the formation is entirely homogeneous, the characteristics of the decreasing distribution curve of the geo-stress are evident from the well wall to the outer boundary.

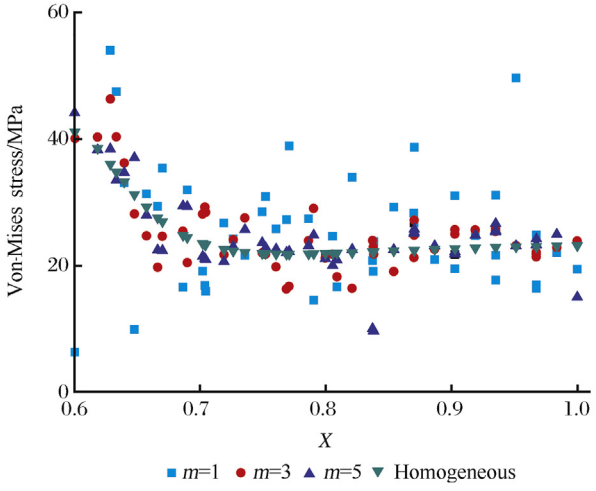

Fig. 5. The von − Mises stress distribution curves at different levels of shape parameters.

4.2. The influence of heterogeneity on strain energy density

When an external force elastically deforms the rock, strain energy is accumulated inside it. The strain energy accumulated per unit volume of rock is called strain energy density. Therefore, the strain energy density plane distribution map at different levels of degrees of heterogeneity with the homogeneous formation and different shape parameters $m = 1$, 3, and 5 are simulated (Fig. 6). Similar to the law of geo-stress distribution, if the formation is homogeneous, the strain energy density is mainly concentrated near the wellbore under the action of flow pressure on the wellbore. In the occasion that the shape parameter *m* changes from one to five, the formation heterogeneity gradually decreases. The formation

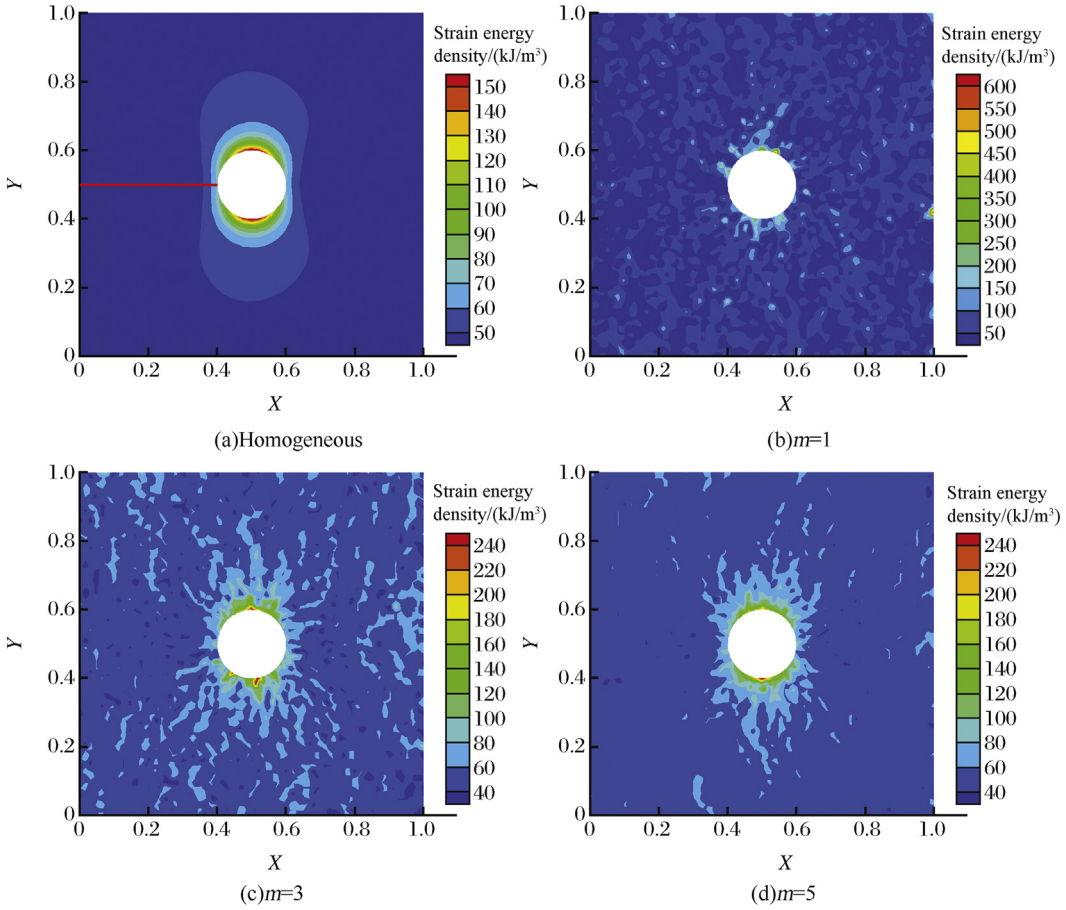

Fig. 6. The 2D distribution figure of strain energy density at different levels of shape parameters *m*.

heterogeneity in Fig. 6b and c is stronger than others, and the high strain energy density appears near the wellbore. In Fig. 6c, the heterogeneity is relatively weak, and the strain energy density is mainly concentrated near the wellbore similarly to Fig. 6a. It indicates that when the shale mechanical heterogeneity is substantial, there is a high strain energy density zone away from the wellbore. Also, the rock damage or fracture probability will increase.

According to the results shown in Fig. 6, along the *x*-axis forward direction as shown by the red line path in Fig. 6a, the strain energy density distribution maps at different levels of shape parameters *m* are plotted (Fig. 7). The formation heterogeneity is strong, and the strain energy exhibits fluctuation characteristics along the path from the borehole wall to the right boundary when $m = 1$. With the increase of the *m* value, the heterogeneity of the formation is weakened, and the strain energy density gradually decreases. When the formation is entirely homogeneous, the strain energy density apparently decreases the distribution curve from the well wall to the outer boundary.

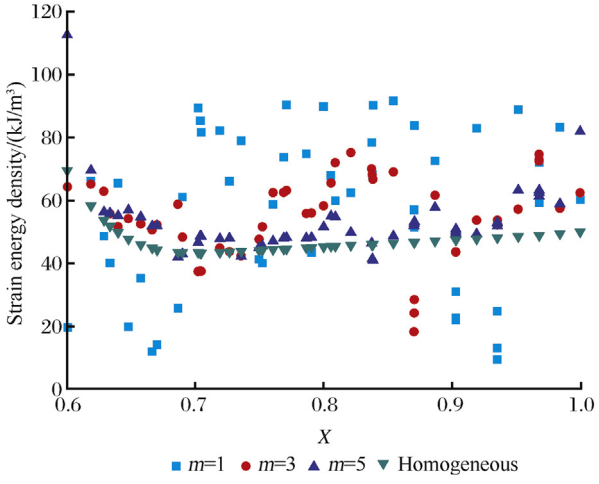

Fig. 7. The strain energy density distribution curves at different levels of shape parameters.

4.3. The influence of heterogeneity on fluid pressure

The pore pressure plane distribution map at different levels of heterogeneous degrees, with the homogeneous formation and the different shape parameters $m = 1$, 3 and 5, is respectively simulated as presented in Fig. 8. Under the action of fluid pressure on the wellbore, if the formation is homogeneous, damage occurs near the wellbore. Moreover, the closer it is to the wellbore, the greater the pore pressure. When

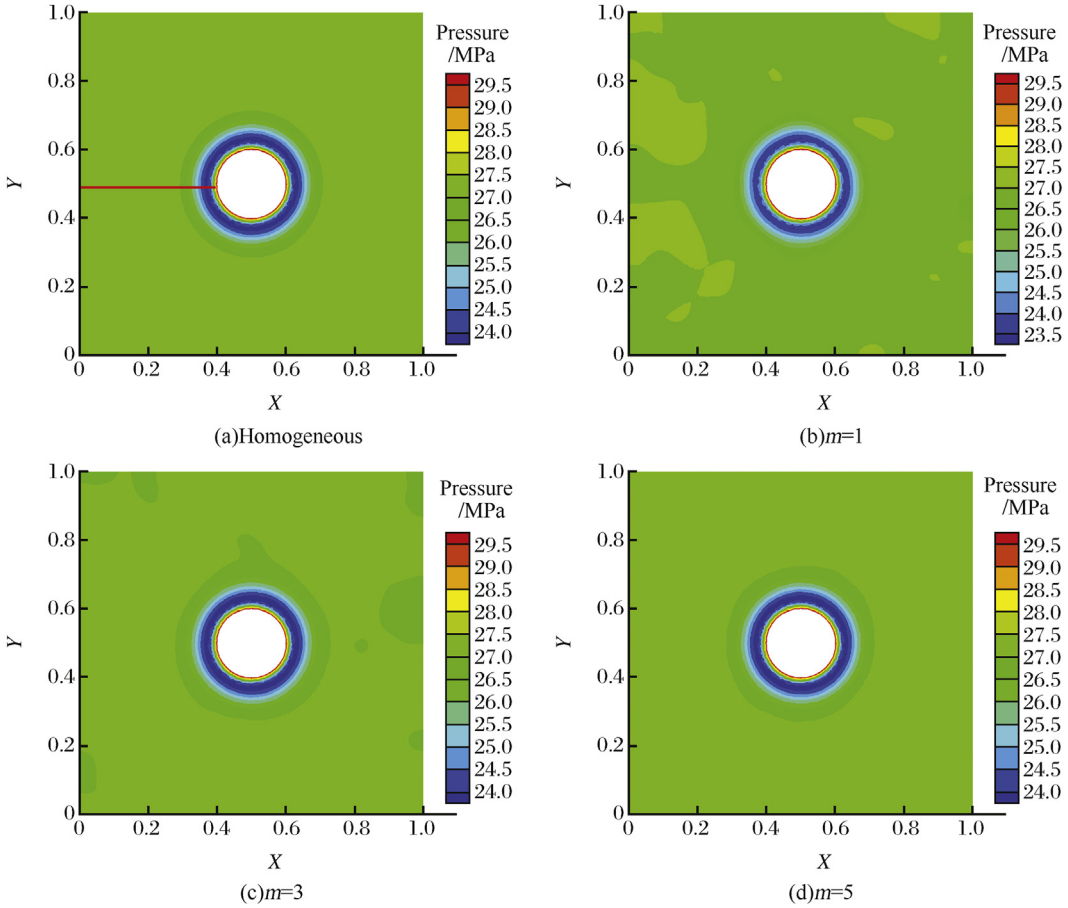

Fig. 8. The 2D distribution figure of pore-pressure at different levels of shape parameters *m*.

the shape parameter *m* changes from one to five, the formation heterogeneity gradually decreases. The formation heterogeneity in Fig. 8b and c is much stronger, and the higher pore pressure occurs near the wellbore. In Fig. 8c, the heterogeneity is relatively weak, and the pore pressure near the wellbore is higher, which is similar to Fig. 8a. The aforementioned indicates that when the shale mechanical heterogeneity is great, there is a high flow pressure zone away from the wellbore. Additionally, the probability of rock damage or fracture will increase.

According to the results of Fig. 8, along the *x*-axis forward direction, as shown by the red line path in Fig. 8a, the strain energy density distribution maps at different levels of shape parameters *m* are plotted as can be seen in Fig. 9. Under the different *m* shape parameters, the flow pressure exhibits a decreasing feature along the path from the well wall to the right boundary. The above corresponds to the distribution in Fig. 8 along the referred path, the formation homogeneity is good. Moreover, there is a small influence of flow pressure distribution on the shape parameter *m*.

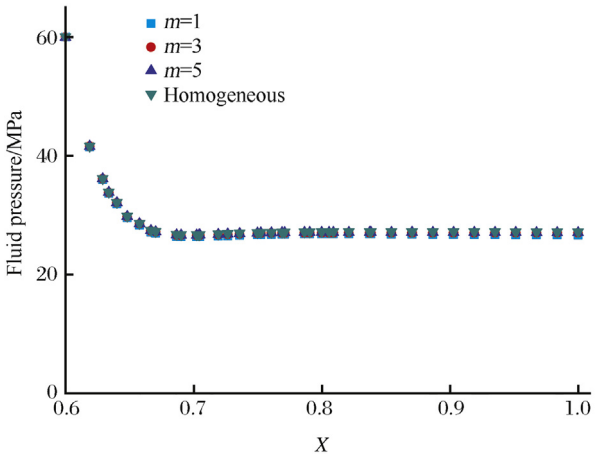

Fig. 9. The fluid pressure distribution curves at different levels of shape parameters.

4.4. The influence of heterogeneity on rock damage

The damage factor plane distribution at different levels of degrees of heterogeneity with the homogeneous formation and different shape parameters m = 1, 3 and 5 is simulated according to Eq. (20) and Eq. (21) as can be observed in Fig. 10. If the formation is homogeneous, damage occurs near the wellbore under the action of flow pressure on the wellbore. Basically, the closer it is to the wellbore, the higher the degree of rock damage. When the shape parameter *m* changes from one to five, the formation heterogeneity gradually decreases.

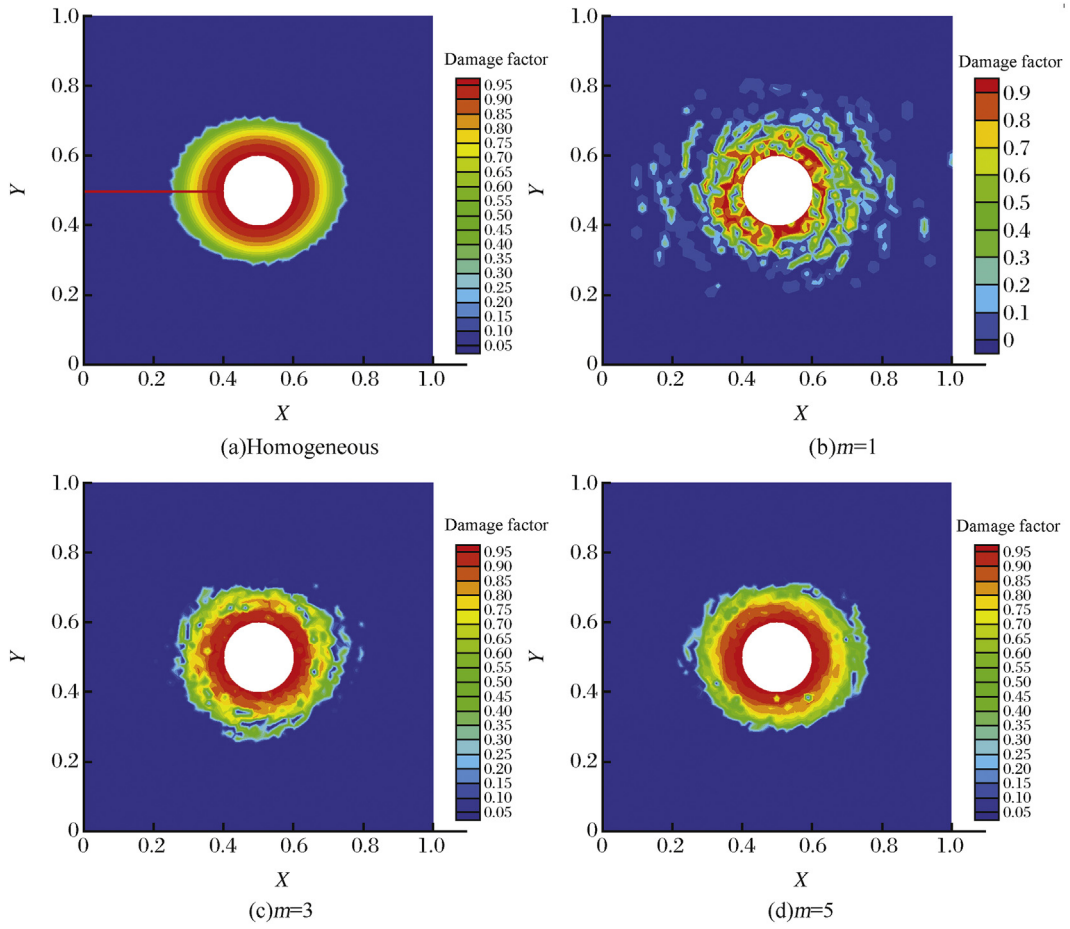

Fig. 10. The 2D distribution figure of damage factors at different levels of shape parameters *m*.

The formation heterogeneity in Fig. 10b and c is much stronger. The different degrees of rock damage appear near the wellbore. In Fig. 10c, the heterogeneity is relatively weak, and the damage is mainly concentrated near the wellbore similar to Fig. 10a. The above shows that the distribution of rock damage under heterogeneous conditions is consistent with the results of stress, strain energy density, and pressure distribution.

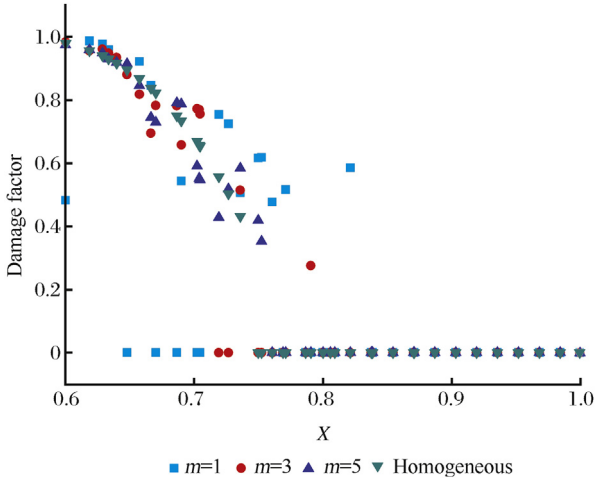

Fig. 11. The damage factor distribution curves at different levels of shape parameters.

According to the results shown in Fig. 10, along the *x*-axis forward direction, as shown by the red line path in Figs. 10a and 11 shows the plotted strain energy density distribution maps at different levels of shape parameters *m*. In the case that $m = 1$, the formation heterogeneity is stronger. The damage factor shows the fluctuation distribution characteristics along the path from the borehole wall to the right boundary. As the *m* value increases, the formation heterogeneity weakens; there is a decreasing trend of the damage factor. When the formation is completely homogeneous, the characteristics of the decreasing distribution curve of the damage factor are obvious from the well wall to the outer boundary.

4.5. The methods for characterization of rock damage/ failure caused by mechanical inhomogeneity and "stress shadow" effect

4.5.1. Von − Mises stress at a single point or line

The -von − Mises stress is the equivalent stress based on shear strain energy. Under certain deformation conditions, the rock yields the variation of elastic potential energy (also called elastic deformation energy) of the rock per unit volume

reaches an absolute constant. It can be seen from the analysis in Section 4.1 that the damage factor has a good correlation with the von – Mises stress. Using the simulation data in Section 4.1, the relationship between the damage factor *D* and the von – Mises stress at different levels of shape parameters *m* is analyzed according to the same path in Fig. 4a (red line); the straight path along the well wall to the right boundary. Shown in Fig. 12 the different levels of shape parameter values where the damage factor has a good correlation with von – Mises stress. The above is validated by the good relationship even when the rock heterogeneity is strong ($m = 1$). As the rock homogeneity increases, the correlation between them becomes stronger. The von – Mises stresses at the single point or line can be used to characterize the local rupture of the rock or the strength of the stress shadow effect.

4.5.2. Strain energy density at a single point or line

The fourth strength theory in material mechanics states that the plastic yield failure of material is caused by the strain energy density (deformation specific energy). Under complex stress state, the material undergoes plastic yield failure when the strain energy density reaches the critical strain energy density of plastic yield failure under uniaxial tension conditions. From the analysis found in Section 4.2, it evident that the damage factor has a good correlation with the strain energy density. The relationship between the damage factor *D* and the strain energy density at different levels of shape parameters *m* is analyzed according to the same path in Fig. 5a (red line); the simulation data is in Section 4.2. The said line is the straight path along the well wall to the right boundary shown in Fig. 13. At different levels of shape parameter values, the damage factor has a good correlation with the strain energy density. Even when the rock heterogeneity is strong ($m = 1$), there is a good relationship between them. It is also worth noting that the correlation between the aforementioned becomes stronger as the rock homogeneity increases. The strain energy density at a single point or line can be used to characterize the local extent of the rock or the strength of the stress shadow effect.

4.5.3. Average strain energy density per unit area

Using the same numerical simulation data, the average strain energy density and the average damage factor at different levels of shape parameters *m* are calculated, and the figures are displayed in Fig. 14. As can be seen observed in Fig. 14a, as the shape parameter m increases, the degree of

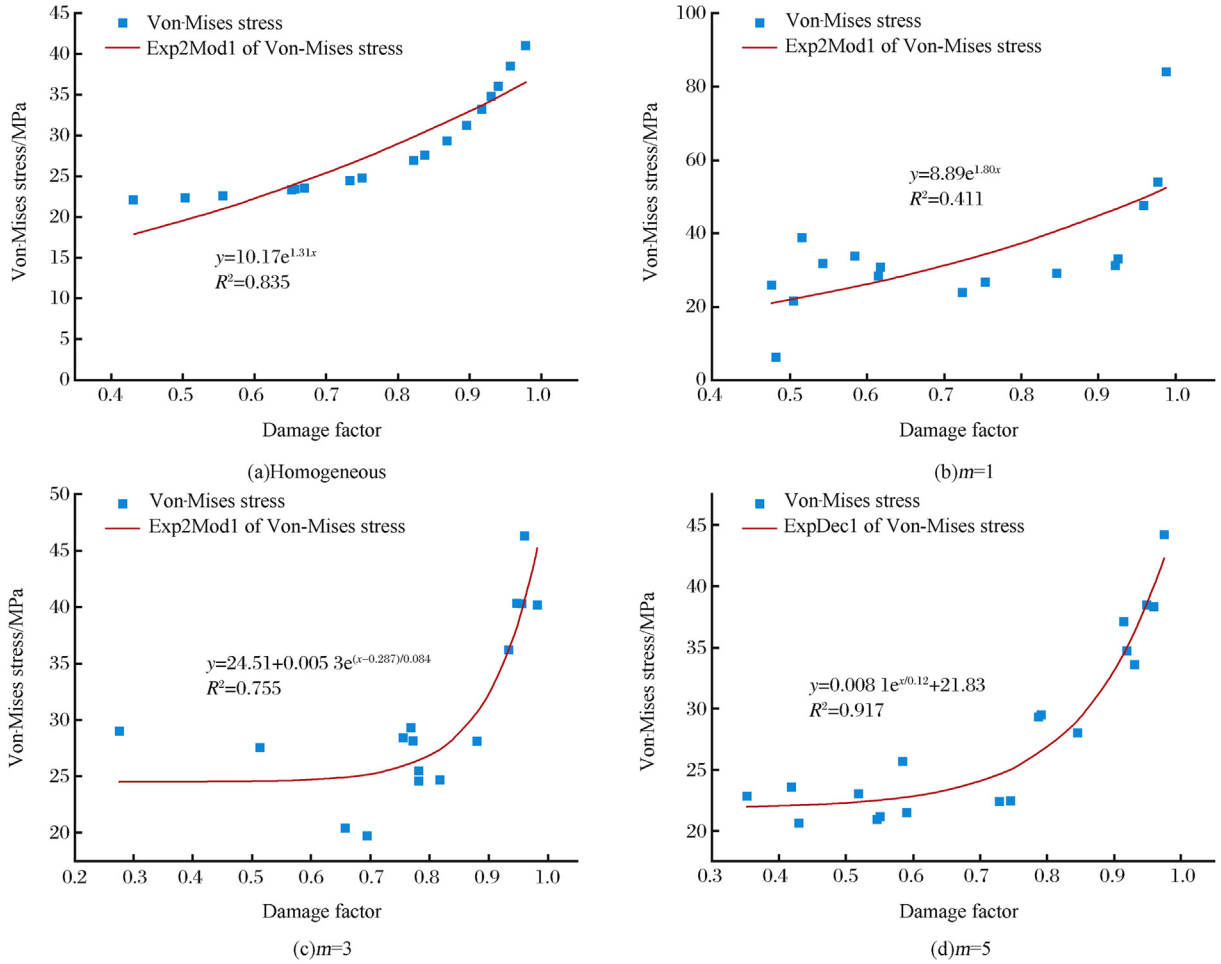

Fig. 12. The relationship curves between the damage factors and the von – Mises stress at different levels of shape parameters *m*.

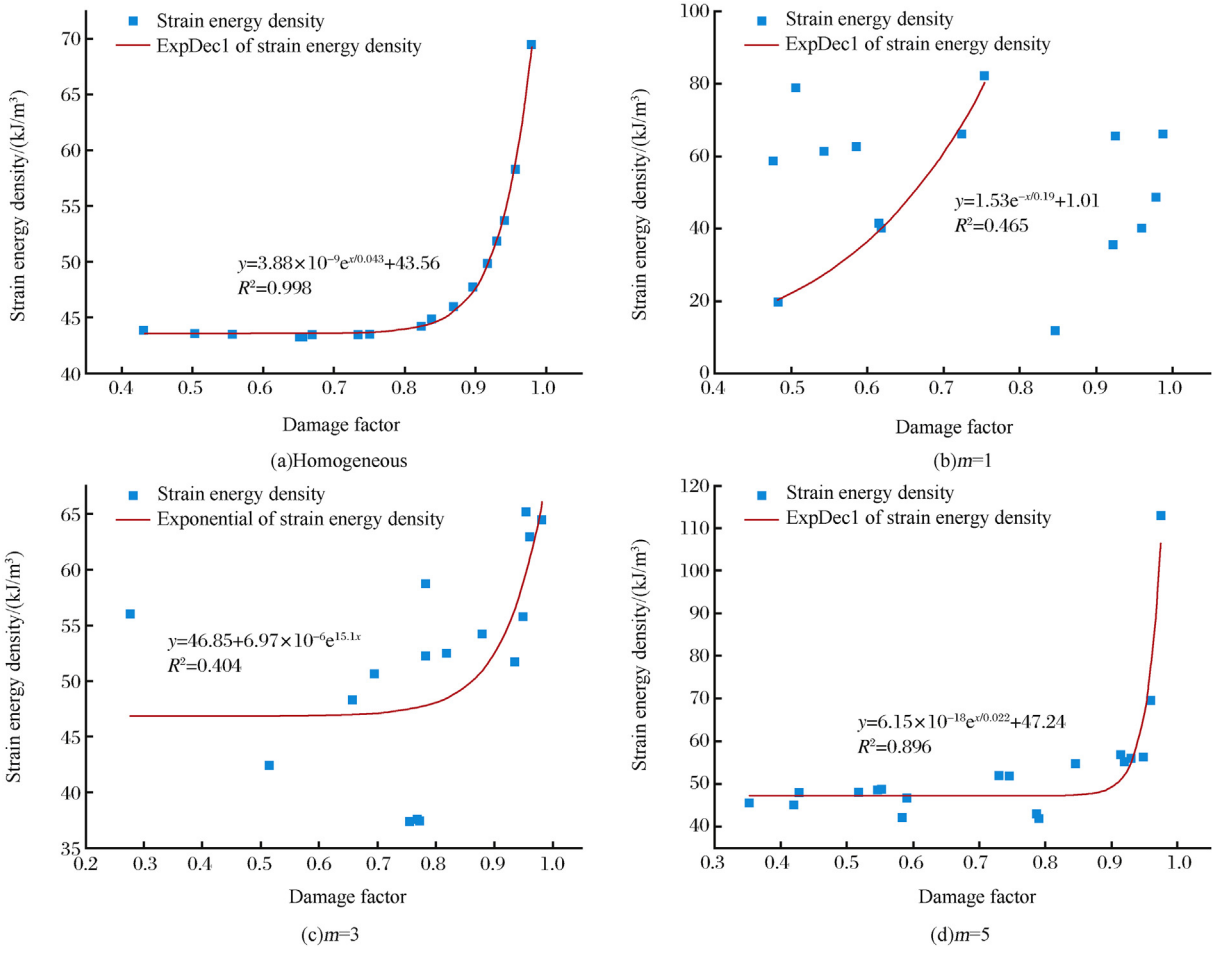

Fig. 13. The relationship curves between damage factors and strain energy density at different levels of shape parameters *m*.

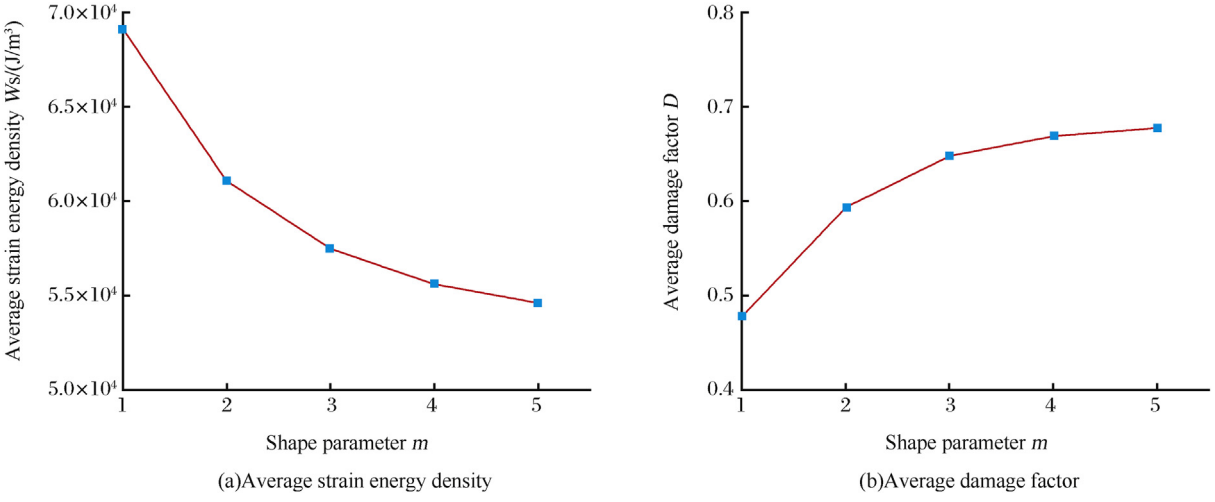

Fig. 14. The relationship curves between the mean value of variables and shape parameter *m*.

heterogeneity gradually decreases, the average strain energy density decreases, and the average damage factor gradually increases. Therefore, the average strain energy density can be used to characterize the damage of the rock after compression. The higher the average strain energy density is, the lower the overall damage degree of the rock. When the degree of heterogeneity is stronger, the lower the average strain energy density in the rock. Hence, the more likely the rock is

damaged. Therefore, the above results are consistent with the fourth strength theory. The average strain energy density can be used to characterize the overall fracture degree of the rock or the strength of the stress shadow effect of the rock.

5. Conclusions

This paper investigates the influence of mechanical heterogeneity on in-situ stress and its damage in gas shale reservoirs by means of a numerical simulation study. Following conclusions can be made in this study:

(1) According to the Galerkin finite element discretization method, the secondary development strategy was successfully done on the geo-stress and rock damage evolution in shale formations through its combination using the COMSOL Multiphysics solver and Matlab scripting language. The Weibull random distribution function was used to represent the mechanical heterogeneity of shale, wherein the corresponding numerical simulation was carried out.
(2) The shape parameter m (the larger the m value, the greater the degree of homogenization) was analyzed for the influence of von − Mises stress, strain energy density, damage factor, and flow pressure. There are obvious characteristics of decreasing distribution of von − Mises stress, strain energy density, and damage factor when the reservoir is completely homogeneous. With the enhancement of formation heterogeneity, their distribution curves show fluctuations. Nonetheless, the damage factor has a good correlation with von − Mises stress and strain energy density.
(3) Under two-dimensional plane strain conditions, a method for characterizing rock damage/fracture and "stress shadow" effect caused by mechanical heterogeneity is proposed. The von − Mises stress or strain energy density at a single point line is used to characterize the local failure degree or the strength of the stress shadow effect of the rock. The average strain energy density per unit area is used to characterize the degree of failure of the rock or the strength of the stress shadow effect.

Funding

Supported by Project of Construction of Innovative Teams and Teacher Career Development for Universities and Colleges Under Beijing Municipality (IDHT20170507); Program of Great Wall Scholar (CIT&TCD20180313); China's Ministry of Science and Technology (973 Program) (2015CB250903); Beijing Postdoctoral Research Foundation (2018-ZZ-045); National Science Foundation of China (51706021); China University of Petroleum (Beijing) in Karamay Campus Scientific Research Fund (RCYJ-2016B-01-001).

Conflict of interest

The authors declare no conflict of interest.

Nomenclature and units

P_w	Bottom hole pressure, MPa
k	Permeability, mD
w	Fracture opening, m
$\boldsymbol{\sigma}$	Stress tensor, MPa·m$^{0.5}$
$\boldsymbol{\varepsilon}$	Strain tensor, dimensionless
ρ	Rock density, kg/m^3
φ	Rock porosity, dimensionless
$\boldsymbol{g}$	Gravitational acceleration, m/s^2
$\boldsymbol{u}$	Displacement vector, m
D	Damage factor, dimensionless
μ_w	Apparent viscosity of fluid, mPa·s
E	Young's modulus, GPa
ν	Poisson's ratio, dimensionless
σ_H	The maximum horizontal principle stress, MPa
σ_h	The minimum horizontal principle stress, MPa
m	Shape parameter, dimensionless
n	Average value of E, GPa
f_{c0}	Uniaxial compressive strength, MPa
f_{t0}	Tensile strength, MPa
ϕ	Internal friction angle
q	Flow rate, m^3/min
t	Injection time, min
K_s, K_w	Bulk modulus of solid particle and fluid, GPa
r_w	Hole radius, m
c_w	Fluid compressibility

References

[1] Wancheng Zhu, Chenhui Wei, Jun Tian, Tianhong Yang, Chun'an Tang, Coupled thermal-hydraulic-mechanical model during rock damage and its preliminary application, Rock Soil Mech. 30 (12) (2009) 3851−3857.
[2] Chenhui Wei, Damage Model for Coal and Rock under Coupled Thermal-hydraulic-mechanical Conditions and its Applications, Northeastern University, Shenyang, 2012, pp. 13−36.
[3] Yinlong Lu, Lianguo Wang, Numerical modeling of mining-induced fracturing and flow evolution in coal seam floor based on micro-crack growth, J. Min. Saf. Eng. 32 (6) (2015) 889−897.
[4] Yongliang Wang, Zhuo Zhuang, Zhanli Liu, Henglin Yang, Finite element analysis of transversely isotropic rock with mechanical-chemical-damage coupling, Eng. Mech. 30 (1) (2016) 105−113.
[5] Kaihua Mi, Numerical Simulation of Meso-damage and Fracture of Full-graded Concrete, Kunming University of Science and Technology, Kunming, 2015, pp. 78−79.
[6] W.C. Zhu, C.A. Tang, Micromechanical model for simulating the fracture process of rock, Rock Mech. Rock Eng. 37 (1) (2004) 25−56.
[7] J.H. Wang, D. Elsworth, Y. Wu, J.S. Liu, W.C. Zhu, Y. Liu, The influence of fracturing fluids on fracturing processes: a comparison between gas and water, in: American Rock Mechanics Association, 49th US Rock Mechanics/Geomechanics Symposium, American Rock Mechanics Association, California, 2015, pp. 1−9.
[8] Y.L. Lu, D. Elsworth, L.G. Wang, Microcrack-based coupled damage and flow modeling of fracturing evolution in permeable brittle rocks, Comput. Geotech. 49 (2013) 226−244.
[9] J. Pogacnik, D. Elsworth, M. O'Sullivan, J. O'Sullivan, A damage mechanics approach to the simulation of hydraulic fracturing/shearing around a geothermal injection well, Comput. Geotech. 71 (2016) 338−351.
[10] X. Li, J.H. Wang, D. Elsworth, Stress redistribution and fracture propagation during restimulation of gas shale reservoirs, J. Petrol. Sci. Eng. 154 (2017) 150−160.

[11] Y. Wang, Z. Liu, H. Yang, Z. Shao, Z. Zhuang, FE analysis of rock with hydraulic-mechanical coupling based on continuum damage evolution, Math. Probl Eng. 2016 (2016) 1−10.
[12] C.S. Oh, N.H. Kim, Y.J. Kim, J.H. Baek, Y.P. Kim, W.S. Kim, A finite element ductile failure simulation method using stress-modified fracture strain model, Eng. Fract. Mech. 78 (1) (2011) 124−137.
[13] T. Gasch, A. Ansell, Cracking in quasi-brittle materials using isotropic damage mechanics, in: Comsol, 2016 Comsol Conference, Munich, 2016, pp. 1−25.
[14] W.D. Wang, G.Y. Zhao, Y.L. Su, Z.T. Feng, Application of network fracturing technology to tight oil reservoirs, Xinjing Pet. Geol. 34 (3) (2013) 345−348.
[15] W.D. Wang, Y.L. Su, L.J. Mu, M.R. Tang, L. Gao, Influencing factors of stimulated reservoir volume of vertical wells in tight oil reservoirs, J. China Univ. Pet. 37 (3) (2013) 93−97.
[16] J. Zhang, D. Zhu, A.D. Hill, Water-induced damage to propped-fracture conductivity in shale formations, SPE Prod. Oper. 31 (2) (2016) 147−156.
[17] J. Zhang, L. Ouyang, D. Zhu, A.D. Hill, Experimental and numerical studies of reduced fracture conductivity due to proppant embedment in the shale reservoir, J. Petrol. Sci. Eng. 130 (2015) 37−45.
[18] J. Zhang, D. Zhu, A.D. Hill, A new theoretical method to calculate shale fracture conductivity based on the population balance equation, J. Petrol. Sci. Eng. 134 (2015) 40−48.
[19] J. Zhang, A. Kamenov, D. Zhu, A.D. Hill, Measurement of realistic fracture conductivity in the Barnett shale, J. Unconv. Oil Gas Resour. 11 (2015) 44−52.